Supplementary information (SI)

Effect of Various Structure Directing Agents (SDAs) on Low-Temperature Deactivation of Cu/SAPO-34 During NH_3-SCR Reaction

Jungwon Woo,[a]* Kirsten Leistner,[a] Diana Bernin,[a] Homayoun Ahari,[b] Mark Shost,[b] Michael Zammit,[b] and Louise Olsson[a]*

[a]*Chemical Engineering, Competence Centre for Catalysis, Chalmers University of Technology, 412 96 Gothenburg, Sweden*

[b]*Fiat Chrysler Automobile US (FCA USA LLC), 800 Chrysler Drive, Auburn Hills, MI 48326-2766, USA*

*jungwon@chalmers.se; *louise.olsson@chalmers.se*

Supplementary figures

Figure S1. SEM image of SAPO-34(MO, TEA, TEAOH, and ACS) and their *average particle size

Figure S2. NOx conversion as a function of temperature on Cu/SAPO-34(TEAOH); reaction conditions: 400 ppm NH_3, 400 ppm NO, 8% O_2, 5% H_2O; GHSV ~24264 h^{-1}

Figure S3. NOx conversion as a function of temperature on Cu/SAPO-34(ACS); reaction conditions: 400 ppm NH_3, 400 ppm NO, 8% O_2, 5% H_2O; GHSV ~24264 h^{-1}

Figure 4. ^{1}H-^{27}Al CP MAS NMR spectra of a) SAPO-34(MO, TEA, TEAOH, ACS), b) Cu/SAPO-34(MO, TEA, TEAOH, ACS)

Figure 5. ^{1}H-^{31}P CP MAS NMR spectra of a) SAPO-34(MO, TEA, TEAOH, ACS), b) Cu/SAPO-34(MO, TEA, TEAOH, ACS)

Figure 6. Ex-situ DRIFT of Cu/SAPO-34(MO, TEA, TEAOH, ACS)

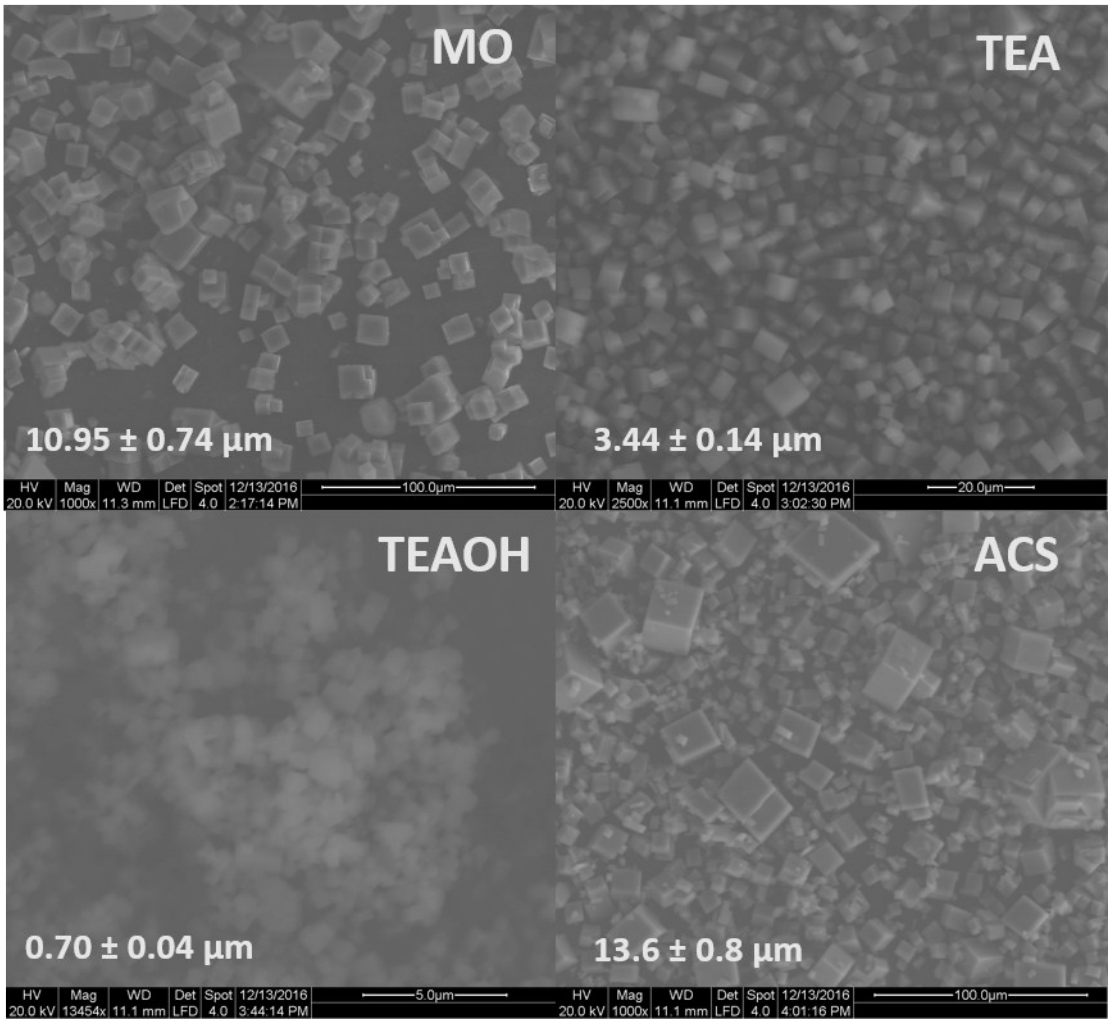

Figure S1. SEM image of SAPO-34(MO, TEA, TEAOH, and ACS) and their *average particle size. *Size of representative 100 particles were measured, and 95 % confidence interval was calculated.

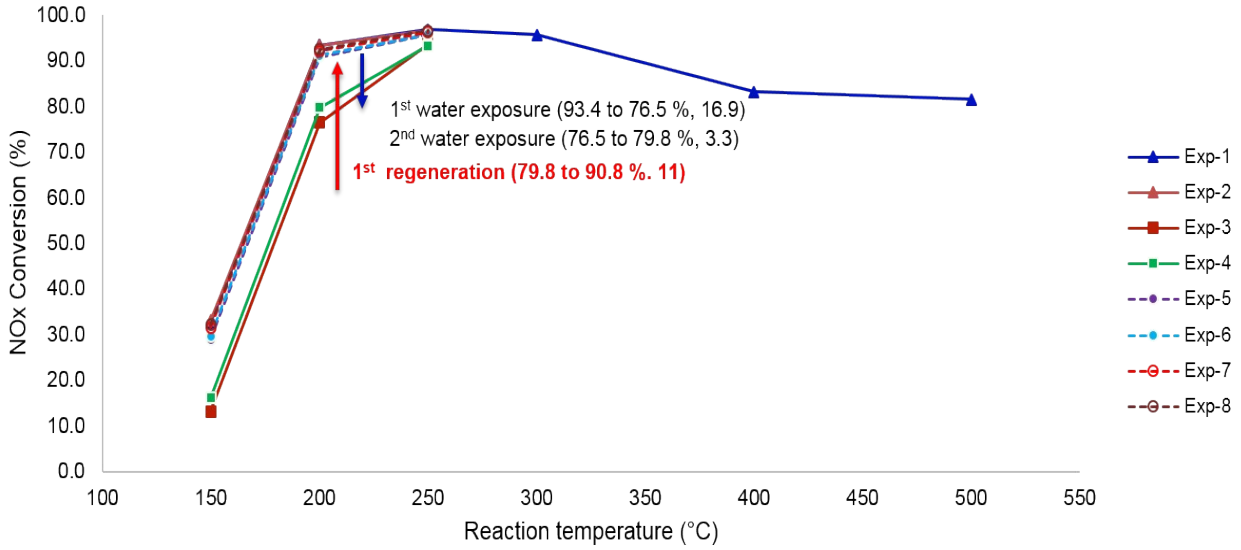

Figure S2. NOx conversion as a function of temperature on Cu/SAPO-34(TEAOH); reaction conditions: 400 ppm NH_3, 400 ppm NO, 8% O_2, 5% H_2O; GHSV ~24264 h^{-1}

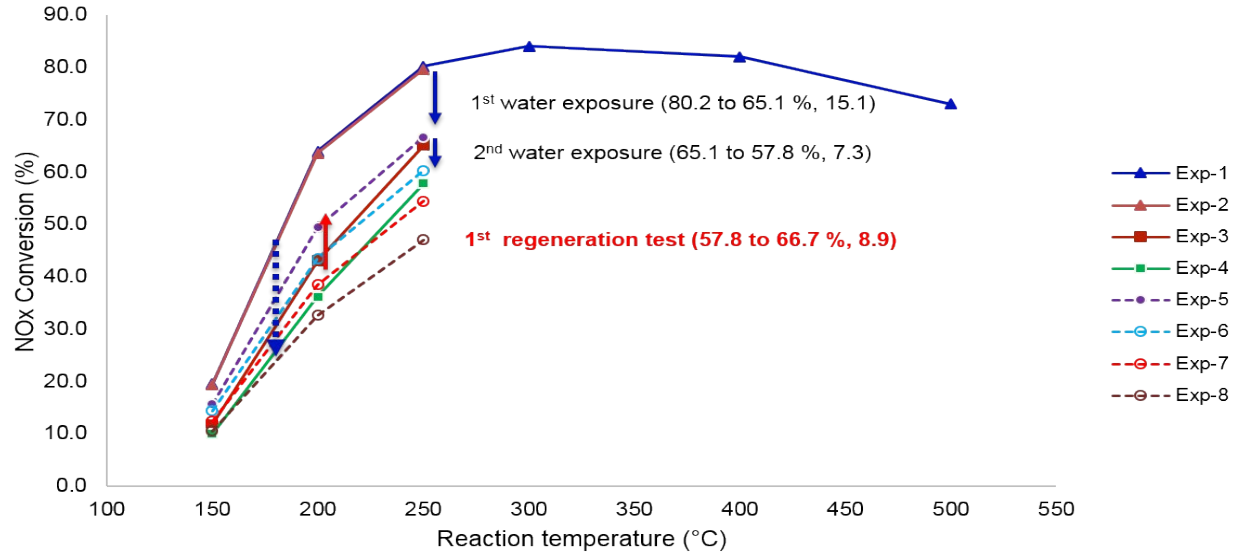

Figure S3. NOx conversion as a function of temperature on Cu/SAPO-34(ACS); reaction conditions: 400 ppm NH_3, 400 ppm NO, 8% O_2, 5% H_2O; GHSV ~24264 h^{-1}

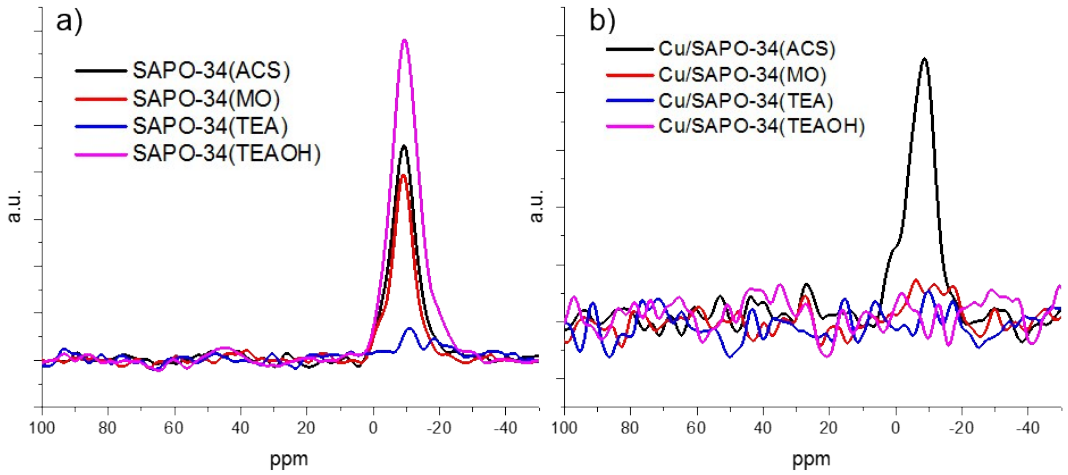

Figure S4. ^{1}H-^{27}Al CP MAS NMR spectra of a) SAPO-34(MO, TEA, TEAOH, ACS), b) Cu/SAPO-34(MO, TEA, TEAOH, ACS)

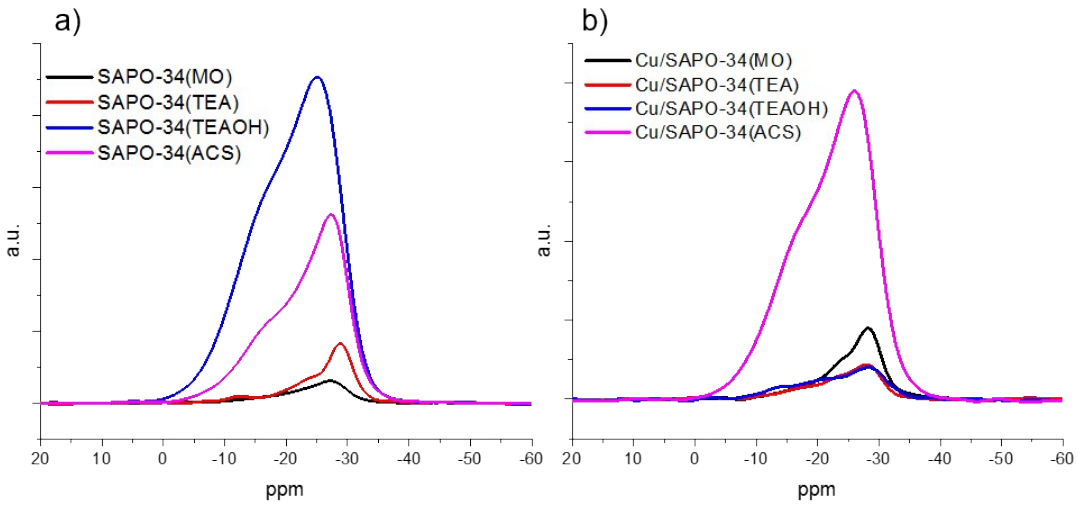

Figure S5. ^{1}H-^{31}P CP MAS NMR spectra [ppm] of a) SAPO-34(MO, TEA, TEAOH, ACS), b) Cu/SAPO-34(MO, TEA, TEAOH, ACS)

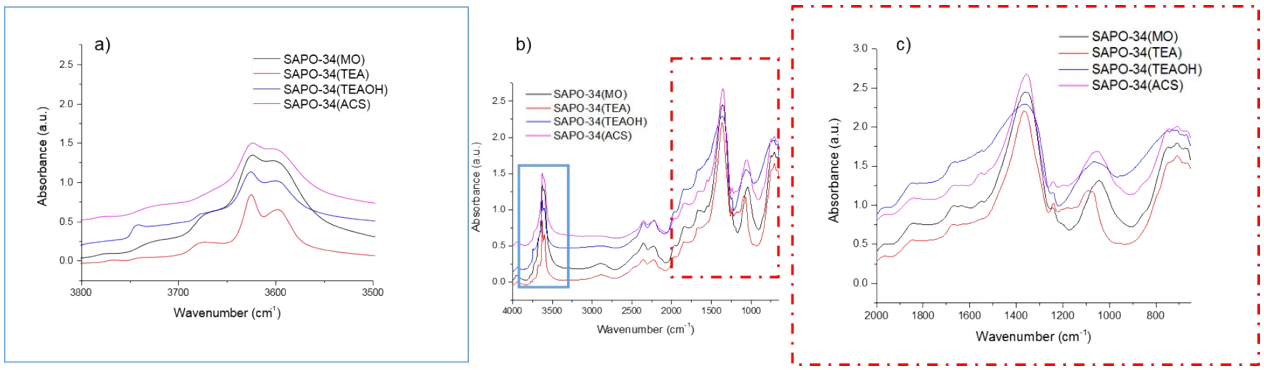

Figure S6. Ex-situ DRIFT of SAPO-34(MO, TEA, TEAOH, ACS)

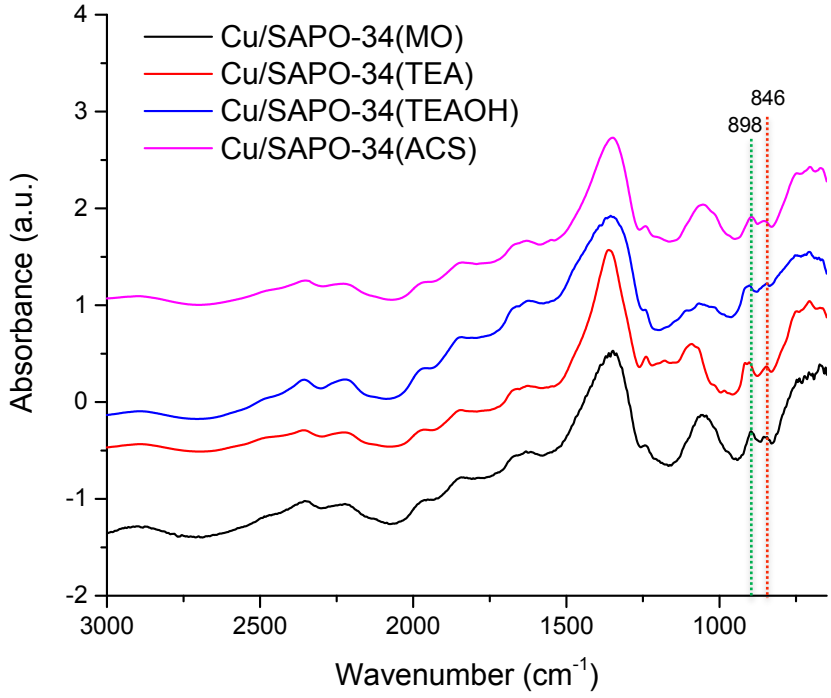

Figure S7. Ex-situ DRIFT of Cu/SAPO-34(MO, TEA, TEAOH, ACS)

Supplementary tables

Table S1. Chemical composition and their relative crystallinity of SAPO-34(MO, TEA, TEAOH)

Table S2. Chemical composition of SAPO-34 and Cu/SAPO-34(MO, TEA, TEAOH, ACS) determined by ICP-SFMS

Table S1. Chemical composition and their relative crystallinity of SAPO-34(MO, TEA, TEAOH)

Catalyst	Molar gel composition					Relative crystallinity*
	Al_2O_3	**P_2O_5**	**SiO_2**	**SDA**	**H_2O**	
SAPO-34(MO)	1	1	1	2	55	100 %
SAPO-34(TEA)	1	1	1	3	55	87.9 %
SAPO-34(TEAOH)	1	1	1	2	55	65.1 %

*Relative crystallinity was calculated based on XRD profiles

Table S2. Chemical composition of SAPO-34 and Cu/SAPO-34(MO, TEA, TEAOH, and ACS) determined by ICP-SFMS

Catalyst	Cu(wt.%)	Si(wt.%)	Al(wt.%)	P(wt.%)
SAPO-34(MO)		5.4	19.7	15.4
SAPO-34(TEA)		5.2	21.1	18.8
SAPO-34(TEAOH)		4.0	17.5	13.9
SAPO-34(ACS)		4.5	16.1	12.8
Cu/SAPO-34(MO)-IWI	1.9	5.6	21.7	15.8
Cu/SAPO-34(TEA)-IWI	1.91	4.2	19.4	16.3
Cu/SAPO-34(TEAOH)-IWI	1.85	5.4	19.8	16.2
SAPO-34(ACS)-IWI	1.86	4.6	15.8	13